AIChE WILEY InterScience DISCOVER SOMETHING GREAT

Control of Gradient Copolymer Composition in ATRP Using Semibatch Feeding Policy

Rui Wang, Yingwu Luo, and Bo-Geng Li
Dept. of Chemical and Biochemical Engineering, State Key Laboratory of Polymer Reaction Engineering, Zhejiang University, Hangzhou, Zhejiang 310017, China

Shiping Zhu
Dept. of Chemical Engineering, McMaster University, Hamilton, Ontario L8S 4L7, Canada

DOI 10.1002/aic.11063
Published online November 30, 2006 in Wiley InterScience (www.interscience.wiley.com).

Controlled/living radical copolymerization (CLRcoP) operated in a batch process is subject to composition drifting and thus produces spontaneous gradient copolymer. The composition distribution along the chain length of individual chains is solely determined by the reactivities of comonomers and the as-synthesized product is uncontrolled. Design of the composition vs. chain length profile provides a new route for developing polymer materials with tailor-made properties. Presented in this article is a theoretical mainframe used for the control over composition distribution along the chain length in atom transfer radical copolymerization. The control is based on a semibatch reactor technology with programmed comonomer feeding rates. Illustrated are three copolymerization model systems with representative reactivity ratios. The targeted composition distribution profiles are uniform, linear gradient, parabolic gradient, hyperbolic gradient, and di-block and tri-block distributions. © 2006 American Institute of Chemical Engineers *AIChE J,* 53: 174–186, 2007
Keywords: gradient copolymer, controlled/living radical polymerization, atom transfer radical polymerization, semibatch reactor, modeling, simulation

Introduction

Controlled/living radical polymerization (CLRP) has been extensively investigated over the past decade.[1–3] There are three well established mechanisms: (1) nitroxide mediated polymerization (NMP),[4–6] (2) atom transfer radical polymerization (ATRP),[7–9] and (3) reversible addition fragmentation chain transfer polymerization (RAFT).[10–12] CLRP is rapidly evolving into a powerful tool in macromolecular engineering.[13,14] CLRP offers great control over molecular weight (MW) and molecular weight distribution (MWD). It has also proved reliable for designing various chain architectures such as block, graft, brush, and star polymers. The majority of work on CLRP in the literature focuses on molecular weight control in homopolymerization, although copolymerization is of particular importance in preparing polymer products with tailored properties.[15–17] By changing the type of comonomers and their relative amounts, a large number of polymer products can be designed. In addition to MW and MWD, copolymer composition (CC) and copolymer composition distribution (CCD) are also key parameters that determine materials properties of a copolymer product. The combination of CLRP and copolymerization, that is, controlled/living radical copolymerization (CLRcoP), provides an opportunity for preparing copolymer products with tailor-made chain structure and superior materials properties.[18–21]

The kinetics of individual chain formation in CLRcoP is very different from that in conventional free radical polymerization. In conventional polymerization, polymer chains are formed instantaneously. It takes only seconds for an individual chain to

Correspondence concerning this article should be addressed to Y. Luo at yingwu.luo@zju.edu.cn or to S. Zhu at zhuship@mcmaster.ca.

propagate thousands of monomers from initiation to termination. The whole course of polymerization usually requires hours to complete with high monomer conversion. The final product is therefore composed of polymer chains generated at different times. Because of the different reactivities of comonomers, polymer chains generated at different times from a batch process have different compositions (that is, "composition drifting"). The copolymer composition is correlated to comonomer composition by the Mayer–Lewis equation. In CLRcoP, the majority of polymer chains are generated at the very beginning of polymerization. The chains remain "living" during the whole course of polymerization at a timescale of hours. The livingness is realized by rapid and frequent exchanges between propagating and dormant states. The chain growth is repeatedly activated and deactivated. All the chains take hours to grow. As a result, the chains are subject to composition drifting from end to end. Individual chains process an identical composition profile. Such a product has been termed a spontaneous gradient copolymer.[7] The synthesis of spontaneous gradient copolymers by batch CLRcoP has been well demonstrated.[18,22,23]

Composition gradient as a new variable to fine-tune chain structure has attracted increased attention in the recent years.[24–26] In theory, the composition gradient can have any profile from uniform to block. The influence of some special composition distributions on polymer properties has been investigated. Gradient copolymers have been found to be more effective than block counterparts in compatibilizing polymer blends. Designing the gradient profile is essential in achieving optimal copolymer properties. In a batch process, the gradient profile is solely determined by the reactivity ratios of comonomers and their initial compositions. For a given pair of comonomers, the gradient profile is spontaneous and as-received. Recently, we launched a research program aimed at developing reactor technologies to design and control optimal gradient copolymer products. In our previous article, we demonstrated by simulation that semibatch RAFT copolymerization with an appropriate monomer feeding policy offers effective control over the copolymer gradient profile.[27] In this work, we develop a kinetic model for semibatch ATRP copolymerization and investigate the effect of comonomer feeding policies on the gradient profile of resulting copolymers.

Model Development

Polymerization scheme and kinetic equations

The elementary reactions involved in the model are summarized in Table 1. In this development, we use the terminal model[28]; that is, only the terminal unit of a propagating radical and the unit adjacent to halogen atom of a dormant chain have influence on the comonomer reactivities. It should be noted that the penultimate effect can be significant in some copolymerization systems.[29] However, taking this effect into account makes the mathematic expressions much more complicated and introduces many kinetic parameters that cannot be easily estimated by experiment. In this article, we also neglect some side reactions, such as thermal self-initiation and β-H elimination by deactivator, for instance.

Table 1. Elementary Reactions Involved in ATRP Copolymerization

Initiation	$P_0X + C \overset{k_{a,0}/k_{d,0}}{\longleftrightarrow} P_0^\bullet + XC$
	$P_0^\bullet + M_i \xrightarrow{k_{in,j}} P_{1,i}^\bullet$
Propagation	$P_{r,i}^\bullet + M_j \xrightarrow{k_{p,ij}} P_{r+1,j}^\bullet$
ATRP equilibrium	$P_{r,i}X + C \overset{k_{a,i}/k_{d,i}}{\longleftrightarrow} P_{r,i}^\bullet + XC$
Termination	$P_{r,i}^\bullet + P_{s,j}^\bullet \xrightarrow{k_{tc,ij}} P_{s+r}$
	$P_{r,i}^\bullet + P_{s,j}^\bullet \xrightarrow{k_{td,ij}} P_r + P_s$

There are three types of chain species involved in the ATRP copolymerization: (1) propagating radical chain ($P_{r,i}^\bullet$), (2) dormant radical chain ($P_{r,i}X$), and (3) dead chain (P_r). The subscript notation r denotes the length of chain, whereas i stands for the terminal unit of chain. The kinetic equations for each type of chains in a batch reactor are summarized in Table 2.

Definition of chain moments and derivation of moment equations

The methodology used in this study is an extension of Zhu's previous work on ATRP copolymerization.[30–32] The moments of chain species are defined in Table 3. With this definition, we can readily describe the chain properties such as instantaneous copolymer composition, number-average chain length, weight-average chain length, polydispersity index, and molar and weight fractions of dead chains:

$$F_i = \frac{k_{in,i}[P_0^\bullet][M_i] + \sum_j k_{p,ji}R_j^0[M_i]}{\sum_i k_{in,i}[P_0^\bullet][M_i] + \sum_i \sum_j k_{p,ji}R_j^0[M_i]} \tag{1a}$$

Table 2. Kinetic Equations for Each Type of Chain Species

Type of Chains	Mass Balance Equations
Propagating radical	$\frac{d[P_{r,i}^\bullet]}{dt} = \sum_j k_{p,ji}[P_{r-1,j}^\bullet][M_i] - \sum_j k_{p,ij}[P_{r,i}^\bullet][M_j] + k_{a,i}[P_{r,i}X][C] - k_{d,i}[P_{r,i}^\bullet][CX] - \sum_j \sum_s k_{t,ij}[P_{r,i}^\bullet][P_{s,j}^\bullet]$
Dormant	$\frac{d[P_{r,i}X]}{dt} = k_{d,i}[P_{r,i}^\bullet][CX] - k_{a,i}[P_{r,i}X][C]$
Dead	$\frac{d[P_r]}{dt} = \sum_i \sum_j \sum_{s=0}^{r} k_{tc,ij}[P_{s,i}^\bullet][P_{r-s,j}^\bullet] + \sum_i \sum_j \sum_s k_{td,ij}[P_{r,i}^\bullet][P_{s,j}^\bullet]$

Table 3. Definition of Various Chain Moments

Type of Chains	Definition of the Moment
Propagating radical	$R_i^m = \sum_{r=1}^{\infty} r^m [P_{r,i}^{\bullet}]$
Dormant	$Q_i^m = \sum_{r=1}^{\infty} r^m [P_{r,i}X]$
Dead	$D^m = \sum_{r=1}^{\infty} r^m [P_r]$

$$\bar{r}_N = \frac{\sum_i (R_i^1 + Q_i^1 + D^1)}{\sum_i (R_i^0 + Q_i^0 + D^0)} \tag{1b}$$

$$\bar{r}_W = \frac{\sum_i (R_i^2 + Q_i^2 + D^2)}{\sum_i (R_i^1 + Q_i^1 + D^1)} \tag{1c}$$

$$PDI = \frac{\bar{r}_W}{\bar{r}_N} \tag{1d}$$

$$N_{dead} = \frac{D^0}{\sum_i (R_i^0 + Q_i^0 + D^0)} \tag{1e}$$

$$W_{dead} = \frac{D^1}{\sum_i (R_i^1 + Q_i^1 + D^1)} \tag{1f}$$

After some mathematical manipulations, a complete set of moment equations can be derived as summarized in Table 4.

Semibatch reactor model

Our objective is to design and control composition distribution along a copolymer chain through semibatch operations. The feed of reactants affects the mass balances in reactor. We therefore need to develop a reactor model for the semibatch polymerization. A well-mixed isothermal tank reactor is assumed in the current work. Because initiator, activator, and deactivator are in trace amounts, only monomer, solvent, and polymer significantly contribute to volume V and density ρ. The evolution of reaction volume V follows:

$$\frac{dV}{dt} = v_f - \sum_{i=1}^{n} mw_i R_{p,i} \left(\frac{1}{\rho_i} - \frac{1}{\rho_p} \right) V \tag{2}$$

where the first term on the right-hand side, v_f, is the volumetric feeding rate, and the second term is the change in volume as a result of difference in the densities between monomer ρ_i and polymer ρ_p. The evolution of density in the reactor can be obtained through applying mass balance to all entities:

$$\frac{d(V_\rho)}{dt} = v_f \rho_f \tag{3a}$$

that is,

$$\frac{d\rho}{dt} = \frac{v_f \rho_f}{V} - \frac{\rho}{V} \frac{dV}{dt} \tag{3b}$$

where ρ_f is the density of feeding materials. The mass balance equations for species i are

$$\frac{d(VC_i)}{dt} = v_f C_{i,f} + VR_i \tag{4a}$$

that is,

$$\frac{dC_i}{dt} = \frac{1}{V} \left(v_f C_{i,f} - C_i \frac{dV}{dt} \right) + R_i \tag{4b}$$

where C_i and $C_{i,f}$ are the concentrations of species i in the reactor and in the feed, respectively; R_i is the intrinsic reaction rate of species i, as expressed in Table 4.

In the simulation, we use the parameters as summarized in Table 5 and assume 75°C. The ATRP bulk copolymerization recipe is shown in Table 6.

Strategy for chain microstructure control

The moment equations in Table4 for the reaction kinetics and Eqs. 2, 3, and 4 for the reactor operation conditions form a complete set of differential equations for the semibatch ATRP copolymerization. Given the initial conditions and feeding policies, we can obtain the composition profile as well as other important chain characters by numerically solving these ODEs. On the other hand, once a special composition profile or chain structure is targeted, we can solve these equations to obtain the feeding policies. Generally, we can apply a constraint to the ODEs:

$$F_1 = f(\bar{r}_N) \tag{5}$$

This constraint is the targeted profile of copolymer composition (F_1) along the polymer chain ($\bar{r}_N$). The form of function f is designed from the requirements of materials properties in application. For example, f can be designed as a continuous function such as Eq. 6 or 7. The former denotes a uniform composition along the copolymer chain and the latter a linear gradient copolymer, respectively:

$$F_1 = \text{constant} \tag{6}$$

$$\frac{F_1}{\bar{r}_N} = \text{constant} \tag{7}$$

However, f can also be a discontinuous function, as in the following equation, which stands for a block copolymer:

$$\begin{cases} F_1 = 0 & \bar{r}_N \le \dfrac{\bar{r}_{N,\text{targeted}}}{2} \\ F_1 = 1 & \bar{r}_N > \dfrac{\bar{r}_{N,\text{targeted}}}{2} \end{cases} \tag{8}$$

By solving these equations, we can obtain a curve of feeding rate vs. time for the targeted chain structure.

Results and Discussion

Copolymer with uniform composition

In a CLRcoP system with different reactivity ratios, a batch process produces gradient copolymer chains as received. The

Table 4. Differential Moment Equations

Zeroth-order moments (that is, molar concentration of chains)

Radical
$$\frac{dR_i^0}{dt} = k_{in,i}[P_0^\bullet][M_i] + \sum_{j\neq i} k_{p,ji}R_j^0[M_i] - \sum_{j\neq i} k_{p,ij}R_i^0[M_j] + k_{a,i}Q_i^0[C] - k_{d,i}R_i^0[CX] - \sum_j k_{t,ij}R_i^0R_j^0 - k_{t,i0}R_i^0[P_0^\bullet]$$

Dormant
$$\frac{dQ_i^0}{dt} = k_{d,i}R_i^0[CX] - k_{a,i}Q_i^0[C]$$

Dead
$$\frac{dD^0}{dt} = \sum_i\sum_j k_{td,ij}R_i^0R_j^0 + \frac{1}{2}\sum_i\sum_j k_{tc,ij}R_i^0R_j^0 + \sum_i k_{t,i0}R_i^0[P_0^\bullet]$$

First-order moments (that is, molar concentration of monomer units in chains)

Radical
$$\frac{dR_i^1}{dt} = k_{in,i}[P_0^\bullet][M_i] + \sum_j k_{p,ji}R_j^0[M_i] + \sum_{j\neq i} k_{p,ji}R_j^1[M_i] - \sum_{j\neq i} k_{p,ij}R_i^1[M_j] + k_{a,i}Q_i^1[C] - k_{d,i}R_i^1[CX] - \sum_j k_{t,ij}R_i^1R_j^0 - k_{t,i0}R_i^1[P_0^\bullet]$$

Dormant
$$\frac{dQ_i^1}{dt} = k_{d,i}R_i^1[CX] - k_{a,i}Q_i^1[C]$$

Dead
$$\frac{dD^1}{dt} = \sum_i\sum_j k_{t,ij}R_i^1R_j^0 + \sum_i k_{t,i0}R_i^1[P_0^\bullet]$$

Second-order moments

Radical
$$\frac{dR_i^2}{dt} = k_{in,i}[P_0^\bullet][M_i] + \sum_j k_{p,ji}R_j^0[M_i]Y_j^0 + \sum_{j\neq i} k_{p,ji}(R_j^2 + 2R_j^1)[M_i] - \sum_{j\neq i} k_{p,ij}R_i^2[M_j] + k_{a,i}Q_i^2[C] - k_{d,i}R_i^2[CX] - \sum_j k_{t,ij}R_i^2R_j^0 - k_{t,i0}R_i^2[P_0^\bullet]$$

Dormant
$$\frac{dQ_i^2}{dt} = k_{d,i}R_i^2[CX] - k_{a,i}Q_i^2[C]$$

Dead
$$\frac{dD^2}{dt} = \sum_i\sum_j k_{td,ij}R_i^2R_j^0 + \sum_i\sum_j k_{tc,ij}(R_i^2R_j^0 + R_i^1R_j^1) + \sum_i k_{t,i0}R_i^2[P_0^\bullet]$$

Small molecules

Initiator
$$\frac{d[P_0X]}{dt} = k_{d,0}[P_0^\bullet][CX] - k_{a,0}[P_0X][C]$$

Primary radical
$$\frac{d[P_0^\bullet]}{dt} = -\sum_i k_{in,i}[M_i][P_0^\bullet] - k_{d,0}[P_0^\bullet][CX] + k_{a,0}[P_0X][C] - \sum_i k_{t,i0}R_i^2[P_0^\bullet] - 2k_{t,00}[P_0^\bullet]^2$$

Catalyst
$$\frac{d[C]}{dt} = k_{d,0}[P_0^\bullet][CX] - k_{a,0}[P_0X][C] + \sum_i k_{d,i}R_i^0[CX] - \sum_i k_{a,i}Q_i^0[C]$$

Deactivator
$$\frac{d[CX]}{dt} = \frac{d[C]}{dt}$$

Monomer
$$\frac{d[M_i]}{dt} = -k_{in,i}[P_0^\bullet][M_i] - \sum_j k_{p,ji}Y_j^0[M_i]$$

gradient profile is solely determined by the reactivity ratios, which may not be optimal in certain applications. For gradient profiles at will, one can apply semibatch feeding strategies. In this section, we demonstrate a semibatch feeding strategy aimed at uniform composition distribution, designed to control the composition drifting along the copolymer chain through a programmed comonomer feeding rate. Three model systems are selected for simulation as shown in Table 7.

In the semibatch process of interest, the targeted copolymer composition is an equal molar fraction of 0.5. The full amount of the slow comonomer (Monomer 2) is charged to the reactor at the very beginning of polymerization. However, only a part of the fast comonomer (Monomer 1) is initially charged. The initial amount of Monomer 1 is calculated from the Mayo–Lewis equation with the targeted copolymer composition ($F_1 = 0.5$) as shown in column 5 in Table 7. The rest of the fast monomer is stored in a tank and is charged to the reactor during the course of polymerization by a programmed metering pump. With the constraint condition of Eq. 6, the feeding rate vs. time curves for the three model

Table 5. Parameters Used in Simulation

Parameter		Value
Initiation $k_{in,i}$	$k_{in,i}$	2 m^3 mol^{-1} s^{-1}
Homo-propagating	$k_{p,ij}$ $(i = j)$	Depends on model system
Cross-propagating	$k_{p,ij}$ $(i \neq j)$	Depends on reactivity ratios
Activation	$k_{a,i}$[33]	10^{-3} m^3 mol^{-1} s^{-1}
Deactivation	$k_{d,i}$[33]	10^4 m^3 mol^{-1} s^{-1}
Disproportional termination	$k_{td,ij}$[34]	10^5 m^3 mol^{-1} s^{-1}
Combinative termination	$k_{tc,ij}$	0 m^3 mol^{-1} s^{-1}
Density of monomer	ρ_{M_i}	900 kg m^{-3}
Density of polymer	ρ_p	1100 kg m^{-3}
Monomer m.w.	mw_i	0.1 kg mol^{-1}

systems, as shown in Figure 1a, are obtained by solving the full set of ODEs.

Figure 1b shows the copolymer composition profiles (symbols) obtained through such feeding policies. For comparison, we also show their "instantaneous composition" profiles (lines) of the corresponding batch operations, that is, the full amounts of both comonomers are charged to the reactor at the very beginning. In the batch cases, the change of instantaneous composition in System 1 ($r_1 = 0.8$, $r_2 = 0.2$) is minor. F_1 is around 0.5 for the most part of copolymer chains and decreases to 0 only at the very end of polymerization. The composition drifting is significant in System 2 ($r_1 = 2$, $r_2 = 0.5$). The individual chains have 2/3 of Monomer 1 at one end and pure Monomer 2 at the other end. The product is a spontaneous and uncontrolled gradient copolymer. In the case of System 3 ($r_1 = 10$, $r_2 = 0.1$), the composition drifting becomes dramatic. The copolymer chains from the batch polymerization have a quarter of their lengths containing 90% of Monomer 1 at one end and another quarter of their lengths with pure Monomer 2 at the other end. The middle portion of the chains has a steep gradient composition distribution.

In contrast, the semibatch operation with the comonomer feeding rate profiles as shown in Figure 1a offers a good control over the composition drifting. In all three model systems, the compositions remain unchanged at the targeted value of $F_1 = 0.5$ along the chain length. It should be pointed out that both radical concentration and copolymer composition change considerably at the beginning of polymerization. It is difficult to control the composition at this unsteady stage. The feeding of Monomer 1 in our simulation starts after the ATRP system reaches its steady state. As the result, the composition approaches the targeted value after a few monomer units.

The influences of the different operation modes (semibatch vs. batch) on polymerization kinetics, molecular weight development, and accumulation of dead polymer are illustrated in Figures 1c–1f. In the cases of Systems 1 and 2, the polymerization is consummated in 20 h for both batch and semibatch operations. The semibatches are slightly slower than their batch counterparts. However, the rate of semibatch polymerization of System 3 is significantly lower than that of its batch. Only 70% monomer conversion is achieved after 40 h. As shown in Figure 1d, independent from the operation modes and reactivity ratios, the number-average chain length increases linearly with the total monomer conversion except for a small deviation at the beginning. The deviation is explained by the fact that not all the initiator molecules are decomposed at the same time. With respect to the molecular weight distribution, the first two systems are well controlled with the polydispersity index (PDI) values about 1.1 for most of the polymerization period. Slightly higher PDI values are observed in the semibatch operations as shown in Figure 1d. In the case of System 3, the PDI value in the semibatch is unfortunately much higher than that in the batch.

Another important property is the fraction of dead chains that have a negative effect on chain functionalization and extension. This information is also provided in our simulation. The molar fractions of dead chains (N_{dead}) are shown in Figure 1e for the different cases, whereas the weight fractions of dead chains (W_{dead}) are shown in Figure 1f. It can be seen that the fractions of dead chains are <20% by mole and 10% by weight in most cases except for the semibatch operation of System 3.

Table 6. Recipes for the Simulation

Component	Total Amount	Amount in Reactor*
Monomer 1	5 mol	Depends on the targeted composition profile and reactivity ratios
Monomer 2	5 mol	Depends on the targeted composition profile and reactivity ratios
Initiator	1 mol % with respect to the total amount of monomer	All charged to reactor*
Activator	1 mol % w.r.t. total amount of monomer	All charged to reactor

*In all cases, initiator and catalyst are charged to the reactor at the very beginning to avoid the generation of living chains at different stages that could broad molecular weight distribution.

Table 7. Model Systems for Simulation

Model System	Approximate Monomer System[22]	Reactivity Ratios	Homo-propagation Rate Coefficients* (m^3 mol s)[35]	Slow Comonomer Initially Charged to Reactor**
1	Styrene *n*-Butyl acrylate	$r_1 = 0.8$ $r_2 = 0.2$	$k_{p,11} = 0.5$, $k_{p,22} = 20$	50.0%
2	Methyl methacrylate Methyl acrylate	$r_1 = 2$ $r_2 = 0.5$	$k_{p,11} = 1$, $k_{p,22} = 5$	53.2%
3	Methyl methacrylate Vinyl chloride	$r_1 = 10$ $r_2 = 0.1$	$k_{p,11} = 1$, $k_{p,22} = 20$	13.2%

*Approximate values at 348.15 K.
**Mayo–Lewis equation at $F_1 = 0.5$; the comonomers are consumed at an unsteady state.

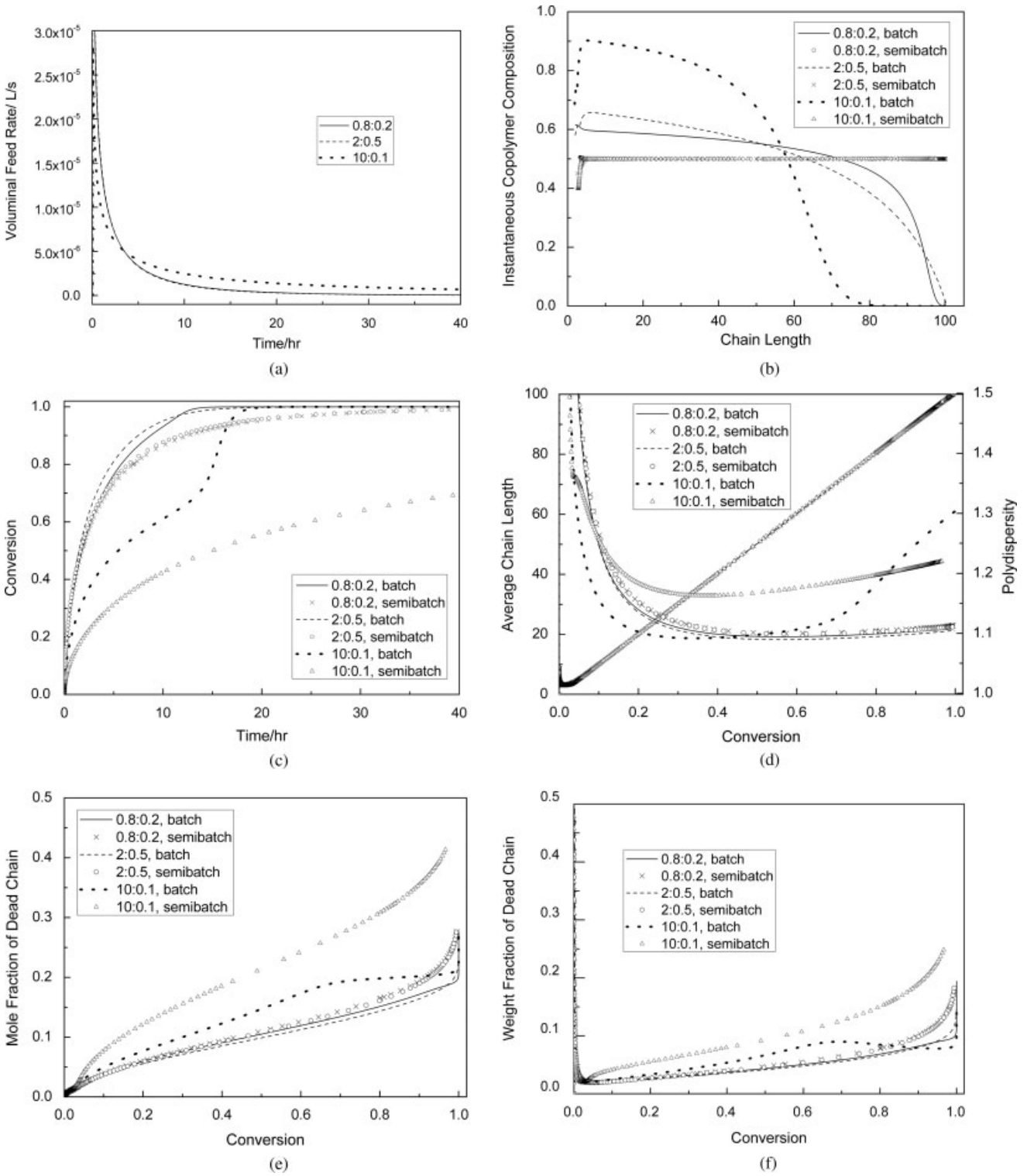

Figure 1. Semibatch ATRP copolymerization of three model systems and targeted uniform copolymer composition $F_1 = 0.5$ (reactivity ratios are noted in the figure).

(a) Variation of volumetric feeding rate with time, (b) instantaneous copolymer composition vs. average chain length, (c) total monomer conversion vs. reaction time, (d) average chain length and polydispersity vs. total monomer conversion, (e) molar fraction of dead chains vs. total monomer conversion, and (f) weight fraction of dead chains vs. total monomer conversion. The lines are the results of a batch operation for comparison.

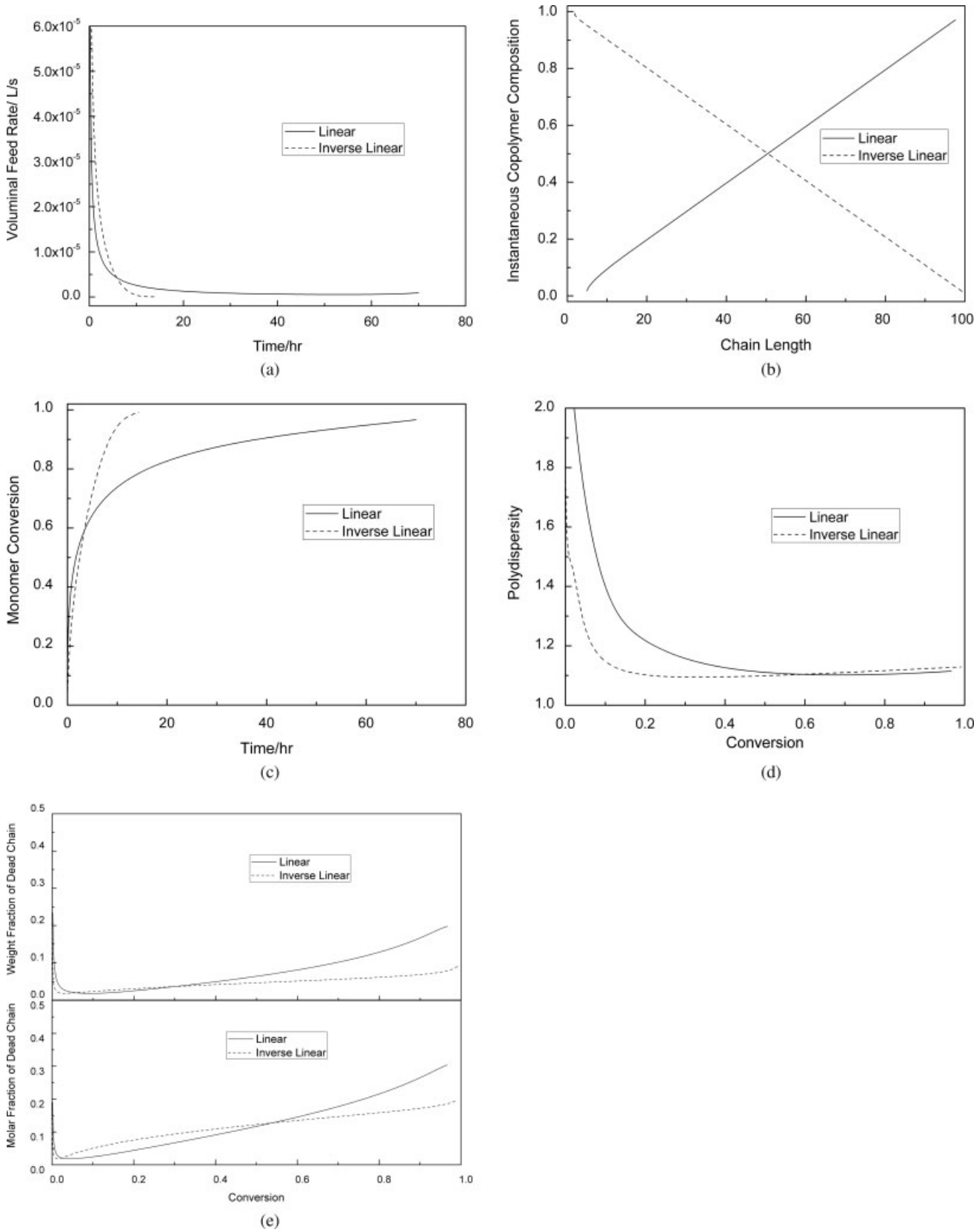

Figure 2. Semibatch ATRP copolymerization with reactivity ratios $r_1 = 2$ and $r_2 = 0.5$ and targeted linear gradient copolymer composition $F_1 = \bar{r}_N/\bar{r}_{N,\text{targeted}}$ and inverse linear gradient copolymer composition $F_1 = 1 - \bar{r}_N/\bar{r}_{N,\text{targeted}}$.

(a) Variation of volumetric feeding rate with time, (b) instantaneous copolymer composition vs. average chain length, (c) total monomer conversion vs. reaction time, (d) average chain length and polydispersity vs. total monomer conversion, and (e) molar and weight fraction of dead chains vs. total monomer conversion.

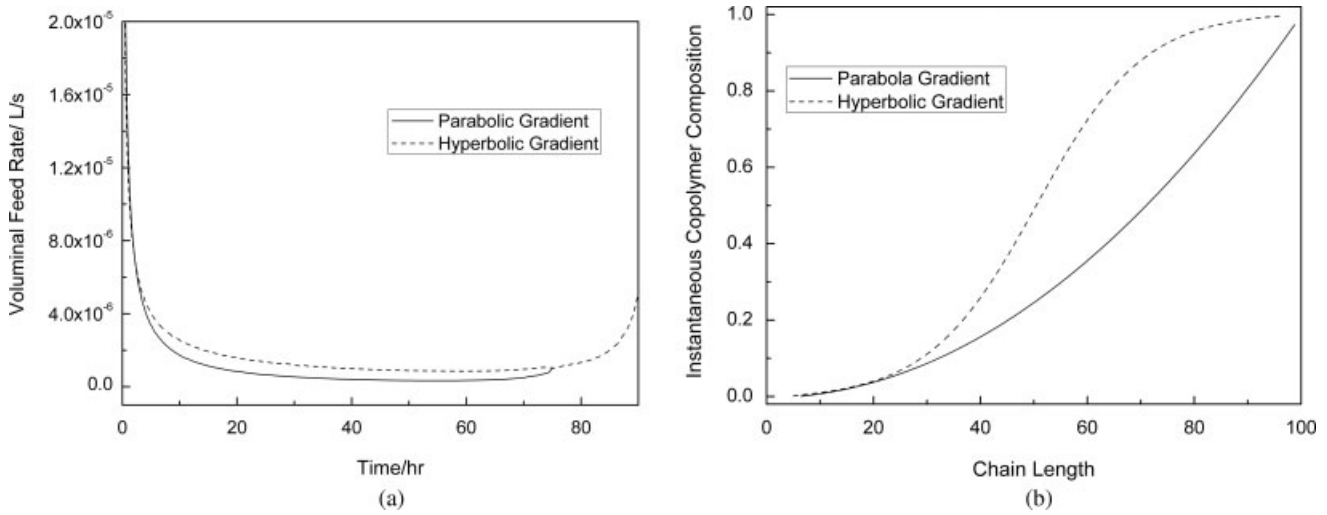

Figure 3. Semibatch ATRP copolymerization with reactivity ratios $r_1 = 2$ and $r_2 = 0.5$ and targeted parabolic and hyperbolic gradient copolymer composition as Eqs. 11 and 12.

(a) Variation of volumetric feeding rate and total monomer conversion with time and (b) instantaneous copolymer composition vs. average chain length.

The model systems we selected for simulation are representative in copolymerization.[36] There are many real systems that have their copolymerization behaviors close to these model systems. From the simulation results, it is found that, unlike the spontaneous and uncontrolled composition drifting in batch operation, the copolymerization in semibatch enjoys good control over copolymer composition along the chain length. However, the semibatch is subject to lower polymerization rates, broader molecular weight distributions, and higher contents of dead chains than its batch counterpart, especially when the difference between reactivity ratios is large.

Gradient copolymers with controlled composition profile

Gradient copolymers have special thermodynamic and mechanical properties, especially interfacial properties, because composition along the chains changes gradually from one end to the other. However, the synthesis of gradient copolymers with controlled composition distribution is still an obstacle for polymer chemists. Besides uniform composition along the chain length, copolymers with controlled gradient composition distributions can also be prepared through semibatch operations. In such cases, the right side of Eq. 5 is a designed function of the average chain length. For example, if a linear gradient copolymer product is targeted, the following expression can be used as the constraint in developing the comonomer feeding strategy:

$$F_1 = \frac{\bar{r}_N}{\bar{r}_{N,\text{targeted}}} \tag{9}$$

For copolymers with an asymmetric composition distribution along chain, there are two approaches in terms of the monomer feeding and direction of chain growth. For example, we can synthesize a linear gradient copolymer by initially charging all Monomer 2 to the reactor and use Eq. 9 to optimize the feeding policy (a normal operation mode). Through the programmed feeding rate of Monomer 1, as shown in Figure 2a, we can obtain the instantaneous copolymer composition that increases linearly from 0 to 1 as the chains grow (see Figure 2b). We can also charge all Monomer 1 to the reactor at the beginning and use the inverse form of Eq. 9

$$F_1 = 1 - \frac{\bar{r}_N}{\bar{r}_{N,\text{targeted}}} \tag{10}$$

to calculate the feeding rate of Monomer 2 (an inverse operation mode). The copolymer composition distribution along chains is shown in Figure 2b. It should be noted that, although the two lines in Figure 2b are inverse with each other, they actually correspond to the same chain structure. The copolymer composition along the chains in Figure 2b deviates from the linear expression when the chains are short in both normal and inverse cases. The slow initiator decomposition rate is responsible for this defect in the chain structure.

The copolymerization kinetics for the linear gradient copolymers are shown in Figure 2c. The polymerization rate of the "inverse" operation mode is much faster than that of the normal mode. The monomer conversion can exceed 95% within 15 h in the former, whereas it requires >60 h in the latter. The PDI values shown in Figure 2d are roughly 1.1 for both cases. However, the fractions of dead chains are quite different, as seen in Figure 2e. At 95% monomer conversion, fractions of the dead chains in the normal and inverse modes are 30 and 18% by mole and 25 and 7% by weight, respectively.

It is interesting to note that the different directions of chain growth have such a dramatic effect on the polymerization rate and dead chain fractions. The inverse mode has a clear advantage over the normal mode in the polymerization rate and product quality in terms of the content of dead chains.

To synthesize gradient copolymers with other novel chain structures, such as parabolic and hyperbolic composition profiles, we can use the following constraint conditions

$$F_1 = \left(\frac{\bar{r}_N}{\bar{r}_{N,\text{targeted}}}\right)^2 \tag{11}$$

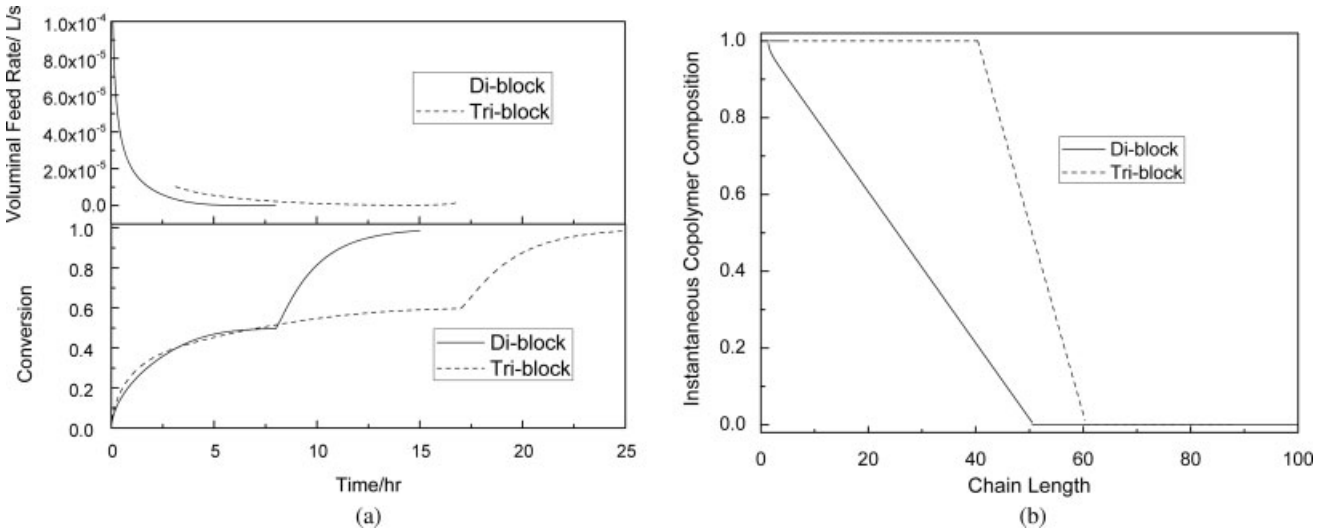

Figure 4. Semibatch ATRP copolymerization with reactivity ratios $r_1 = 2$ and $r_2 = 0.5$ and targeted di-block and tri-block copolymers as Eqs. 13 and 14.

(a) Variation of volumetric feeding rate with time and (b) instantaneous copolymer composition vs. average chain length.

$$F_1 = \frac{1}{2} + \frac{1}{2}\tanh\,\lambda\left(\frac{\bar{r}_N}{\bar{r}_{N,\text{targeted}}} - \frac{1}{2}\right) \tag{12}$$

to obtain the feeding policies. The hyperbolic gradient copolymer described by Eq. 12 has an adjustable parameter λ ($\lambda = 5$ in our simulation) that determines the gradient sharpness. As the λ value increases, this gradient copolymer becomes similar to a di-block structure. The semibatch monomer feeding curves are given in Figure 3a. The instantaneous composition distributions of as-synthesized gradient copolymers are illustrated in Figure 3b.

Di-block and tri-block copolymers

If di-block and tri-block copolymers with a gradient portion are targeted, the expressions of the composition profiles can be set as

$$\begin{cases} F_1 = 1 - \dfrac{2\bar{r}_N}{\bar{r}_{N,\text{targeted}}} & \bar{r}_N \le \dfrac{\bar{r}_{N,\text{targeted}}}{2} \\ F_1 = 0 & \bar{r}_N > \dfrac{\bar{r}_{N,\text{targeted}}}{2} \end{cases} \tag{13}$$

$$\begin{cases} F_1 = 1 & \bar{r}_N \le \dfrac{2\bar{r}_{N,\text{targeted}}}{5} \\ F_1 = 3 - \dfrac{5\bar{r}_N}{\bar{r}_{N,\text{targeted}}} & \dfrac{2\bar{r}_{N,\text{targeted}}}{5} < \bar{r}_N \le \dfrac{3\bar{r}_{N,\text{targeted}}}{5} \\ F_1 = 0 & \bar{r}_N > \dfrac{3\bar{r}_{N,\text{targeted}}}{5} \end{cases} \tag{14}$$

The chain structures are illustrated in Figure 4b. There are two steps to synthesize the di-block copolymer described by Eq. 13. First, charging all Monomer 1 to the reactor and feeding Monomer 2 by a programmed metering pump to generate the linear gradient portion. Then, all Monomer 2 left in the tank is charged to the reactor to advance the polymerization for the generation of homopolymer block. The process to synthesize the tri-block copolymer is different from that of di-block only by adding a step to form a homopolymer block of Monomer 1 at the first. The feed rates for the gradient block are shown in Figure 4a with the polymerization rate profiles. It should be noted that as linear gradient copolymers there are also two directions to synthesize the gradient block in the di-block and tri-block copolymers.

A final point worth mentioning is that the methodology developed in this work is generally applicable, where just a few examples are illustrated. Polymer materials properties are determined by chain microstructures. Designing chain structure such as the copolymer composition distribution is critical for the development of novel polymer materials with tailor-made properties. The semibatch CLRcoP provides a powerful tool for this purpose. As long as the targeted function of composition vs. chain length is defined, the developed semibatch technology can be used for the polymer synthesis through a programmed comonomer feeding strategy. The computation requirement is minimal. In some special cases with certain assumptions, analytical solutions of the ODEs can be obtained. The Appendix shows the uniform composition case as an example.

Conclusions

The recently introduced novel concept of chain microstructure—gradient copolymers—is the result of controlled/living radical copolymerization (CLRcoP). Batch polymerization processes produce spontaneous gradient composition distributions that are solely determined by comonomer reactivity ratios. Copolymer materials with such as-synthesized composition distributions may not be optimal for certain applications. In this work, we developed a mathematical model based on the semibatch atom transfer radical copolymerization (ATRcoP). The model predicts the polymerization rate, composition distribution, molecular weight, polydispersity,

and both number and weight fractions of dead chains. It is demonstrated that precise design and control of various composition distributions along the chain length can be achieved through programmed comonomer feeding rates. Three copolymerization model systems with representative reactivity ratios ($r_1 = 0.8$, $r_2 = 0.2$; $r_1 = 2$, $r_2 = 0.5$; $r_1 = 10$, $r_2 = 0.1$) are theoretically investigated. The example products in the simulation are uniform, linear gradient, parabolic gradient, hyperbolic gradient, and di-block and tri-block copolymers. It is found that in the synthesis of gradient copolymer with an asymmetric composition distribution, the direction of chain growth has a significant effect on both the polymerization rate and the fraction of dead chains. For example, the inverse mode has a clear advantage over the normal mode in the preparation of linear gradient copolymers. A challenge of the semibatch operation can be lower polymerization rate, broader molecular weight distribution, and higher content of dead chains than those of its corresponding batch counterpart, particularly when the reactivity ratios significantly deviate from unity. It should be pointed out that the developed methodology is generally applicable for any targeted distributions.

Acknowledgments

The authors thank the National Science Foundation of China (NSFC) for a JB Award, the Ministry of Education of China for a Changjiang Scholar Visiting Fellowship and for New Century Excellent Talent in University, and Zhejiang University for supporting this research.

Notation

C = activator
C_i = concentration of species i in the reactor, mol m^{-3}
$C_{i,f}$ = concentration of species i in the feed, mol m^{-3}
D^m = mth-order moment of dead chain
F_I = instantaneous copolymer composition
$k_{a,i}$ = activation rate coefficient for dormant chain with i-type of terminal unit, m^3 mol^{-1} s^{-1}
$k_{d,i}$ = deactivation rate coefficient for radical with i-type of terminal unit, m^3 mol^{-1} s^{-1}
$k_{in,i}$ = initiation rate coefficient, m^3 mol^{-1} s^{-1}
$k_{p,ij}$ = propagating rate coefficient for monomer j adding to radical with i-type of terminal unit, m^3 mol^{-1} s^{-1}
$k_{tc,ij}$ = combinative termination rate coefficient between radicals with i and j types of terminal unit, m^3 mol^{-1} s^{-1}
$k_{td,ij}$ = disproportional termination rate coefficient between radicals with i and j types of terminal unit, m^3 mol^{-1} s^{-1}
mw_i = molecular weight of monomer i, kg mol^{-1}
M_i = monomer i
N_{dead} = molar fraction of dead chain
$P_0^{\bullet}$ = primary radical
P_0X = initiator
PDI = polydispersity index
P_r = dead chain with length r
$P_{r,i}^{\cdot}$ = propagating radical chain with length r and i-type of terminal unit
$P_{r,i}X$ = dormant chain with length r and i-type of terminal unit
Q_i^m = mth-order moment of dormant chain with i-type of terminal unit
r_i = reactivity ratio of monomer i
$\overline{r}_N$ = number-average chain length
$\overline{r}_{N,targeted}$ = targeted number-average chain length
$\overline{r}_W$ = weight-average chain length
R_i = intrinsic reaction rate of species i, mol m^{-3} s^{-1}
R_i^m = mth-order moment of propagating radical with i-type of terminal unit
$R_{p,i}$ = intrinsic propagating rate of monomer i, mol m^{-3} s^{-1}
V = reaction volume, m^3
v_f = volumetric feeding rate, m^3 s^{-1}
W_{dead} = weight fraction of dead chain
XC = deactivator

Greek letters

ρ = reaction density, kg m^{-3}
ρ_i = density of monomer i, kg m^{-3}
ρ_p = density of polymer, kg m^{-3}
ρ_f = density of feeding materials, kg m^{-3}

Literature Cited

1. Davis KA, Matyjaszewski K. Statistical, gradient, block and graft copolymers by controlled/living radical polymerizations. *Adv Polym Sci*. 2002;159:1–169.
2. Kamigaito M, Ando T, Sawamto M. Metal-catalyzed living radical polymerization. *Chem Rev*. 2001;101:3689–3745.
3. Goto A, Fukuda T. Kinetics of living radical polymerization. *Prog Polym Sci*. 2004;29:329–385.
4. Georges MK, Veregin RPN, Kazmaier PM, Hamer GK. Narrow molecular weight resins by a free-radical polymerization process. *Macromolecules*. 1993;26:2987–2988.
5. Moad G, Rizzardo E, Solomon DH. Selectivity of the reaction of free radicals with styrene. *Macromolecules*. 1982;15:909–914.
6. Hawker CJ, Bosman AW, Harth E. New polymer synthesis by nitroxide mediated living radical polymerizations. *Chem Rev*. 2001;101:3661–3688.
7. Matyjaszewski K, Xia JH. Atom transfer radical polymerization. *Chem Rev*. 2001;101:2921–2990.
8. Matyjaszewski K, Gaynor S, Wang JS. Controlled radical polymerizations: The use of alkyl iodides in degenerative transfer. *Macromolecules*. 1995;28:2093–2095.
9. Faucher S, Okrutny P, Zhu S. Facile and effective purification of polymers produced by atom transfer radical polymerization via simple catalyst precipitation and microfiltration. *Macromolecules*. 2006;39:3–5.
10. Chiefari J, Chong YK, Ercole F, Krstina J, Jeffery J, Le TPT, Mayadunne RTA, Meijs GF, Moad CL, Moad G, Rizzardo E, Thang SH. Living free-radical polymerization by reversible addition-fragmentation chain transfer: The RAFT process. *Macromolecules*. 1998;31:5559–5562.
11. Feldermann A, Coote ML, Martina HP, Stenzel H, Davis TP, Barner-Kowollik C. Consistent experimental and theoretical evidence for long-lived intermediate radicals in living free radical polymerization. *J Am Chem Soc*. 2004;126:15915–15923.
12. Luo Y, Wang R, Yang L, Yu B, Li B, Zhu S. Effect of reversible addition-fragmentation transfer (RAFT) reactions on (mini)emulsion polymerization kinetics and estimate of RAFT equilibrium constant. *Macromolecules*. 2006;39:1328–1337.
13. Matyjaszewski K. Macromolecular engineering: From rational design through precise macromolecular synthesis and processing to targeted macroscopic material properties. *Prog Polym Sci*. 2005;30:858–875.
14. Perrier S, Takolpuckdee P. Macromolecular design via reversible addition-fragmentation chain transfer (RAFT)/xanthates (MADIX) polymerization. *J Polym Sci Part A: Polym Chem*. 2005;43:5347–5393.
15. Sikka M, Pellegrini NN, Schmitt EA, Winey KI. Modifying a polystyrene/poly(methyl methacrylate) interface with poly(styrene-co-methyl methacrylate) random copolymers. *Macromolecules*. 1997;30;445–455.
16. Kulasekere R, Kaiser H, Ankner JF, Russell TP, Brown HR, Hawker CJ, Mayes AM. Homopolymer interfaces reinforced with random copolymers. *Macromolecules*. 1996;29:5493–5496.
17. Dadmum M. Effect of copolymer architecture on the interfacial structure and miscibility of a ternary polymer blend containing a copolymer and two homopolymers. *Macromolecules*. 1996;29:3868–3874.
18. Luo Y, Liu XZ. Reversible addition-fragmentation transfer (RAFT) copolymerization of methyl methacrylate and styrene in miniemulsion. *J Polym Sci Part A: Polym Chem*. 2004;42:6248–6258.
19. Zeng F, Shen Y, Zhu S. Synthesis of comb-branched polyacrylamide with cationic poly[(2-dimethylamino)ethyl methacrylate dimethylsulfate] quat. *J Polym Sci Part A: Polym Chem*. 2002;40:2394–2405.

20. Shinoda H, Matyjaszewski K. Improving the structural control of graft copolymers. Copolymerization of poly(dimethylsiloxane) macromonomer with methyl methacrylate using RAFT polymerization. *Macromol Rapid Commun*. 2001;22:1176–1181.
21. Shinoda H, Matyjaszewski K, Okrasa L, Mierzwa M, Pakula T. Structural control of poly(methyl methacrylate)-*g*-poly(dimethylsiloxane) copolymers using controlled radical polymerization: Effect of the molecular structure on morphology and mechanical properties. *Macromolecules*. 2003;36:4772–4778.
22. Matyjaszewski K, Ziegler MJ, Arehart SV, Greszta D, Pakula T. Gradient copolymers by atom transfer radical copolymerization. *J Phys Org Chem*. 2000;13:775–786.
23. Ziegler MJ, Matyjaszewski K. Atom transfer radical copolymerization of methyl methacrylate and *n*-butyl acrylate. *Macromolecules*. 2001;34:415–424.
24. Shull KR. Interfacial activity of gradient copolymers. *Macromolecules*. 2002;35:8631–8639.
25. Lefebvre MD, Olvera de la Cruz, Shull KR. Phase segregation in gradient copolymer melts. *Macromolecules*. 2004;37:1118–1123.
26. Gray MK, Zhou H, Nguyen ST, Torkelson JM. Synthesis and glass transition behavior of high molecular weight styrene/4-acetoxystyene and styrene/4-hydroxystyrene gradient copolymers made via nitroxide-mediated controlled radical polymerization. *Macromolecules*. 2004;37:5586–5595.
27. Wang R, Luo Y, Li B, Sun X, Zhu S. Design and control of copolymer composition distribution in living radical polymerization using semi-batch feeding policies: A model simulation. *Macromol Theory Simul*. 2006;15:356–368.
28. Merz E, Alfrey T, Goldfinger G. Intramolecular reactions in vinyl polymers as a means of investigation of the propagation step. *J Polym Sci*. 1946;1:75–82.
29. Coote ML, Davis TP. The mechanism of the propagation step in free-radical copolymerization. *Prog Polym Sci*. 1999;24:1217–1251.
30. Zhu S. Modeling stable free-radical polymerization. *J Polym Sci Part B: Polym Phys*. 1999;37:2692–2704.
31. Zhu S. Modeling of molecular weight development in atom transfer radical polymerization. *Macromol Theory Simul*. 1999;8:29–37.
32. Wang A, Zhu S. Modeling the reversible addition-fragmentation transfer polymerization process. *J Polym Sci Part A: Polym Chem*. 2003;41:1553–1566.
33. Matyjaszewski K. Structure–reactivity correlation in atom transfer radical polymerization. *Macromol Symp*. 2002;182:209–224.
34. Beuermann S, Buback M. Rate coefficients of free-radical polymerization deduced from pulsed laser experiments. *Prog Polym Sci*. 2002;27:191–254.
35. Odian G. Principle of Polymerization. 4th Edition. Hoboken, NJ: Wiley; 2004.
36. Brandrup J, Immergut E, Grulke E, eds. Polymer Handbook. 4th Edition. New York:Wiley; 1999.
37. Charleux B, Nicolas J, Guerret O. Theoretical expression of the average activation-deactivation equilibrium constant in controlled/living free-radical copolymerization operating via reversible termination. Application to a strongly improved control in nitroxide-mediated polymerization of methyl methacrylate. *Macromolecules*. 2005;38:5485–5492.
38. Fischer H. The persistent radical effect in controlled radical polymerizations. *J Polym Sci Part A: Polym Chem*. 1999;37:1885–1901.
39. Tang W, Tsarevsky NV, Matyjaszewski K. Determination of equilibrium constants for atom transfer radical polymerization. *J Am Chem Soc*. 2006;128:1596–1604.

Appendix: Analytical Expression for the Kinetics of Synthesizing Uniform Copolymer

Based on the previous theoretical work of Charleux et al.,[37] the pseudokinetic rate coefficients for ATRP copolymerization can be expressed as follows:

Propagation

$$\langle k_p \rangle = k_{p11}\phi_1 f_1 + k_{p21}\phi_2 f_1 + k_{p12}\phi_1 f_2 + k_{p22}\phi_2 f_2 \qquad \text{(A1)}$$

Termination

$$\langle k_t \rangle = k_{t11}\phi_1^2 + 2k_{t12}\phi_1\phi_2 + k_{t22}\phi_2^2 \qquad \text{(A2)}$$

Deactivaton

$$\langle k_d \rangle = k_{d1}\phi_1 + k_{d2}\phi_2 \qquad \text{(A3)}$$

Activation

$$\langle k_a \rangle = k_{a1}\psi_1 + k_{a2}\psi_2 \qquad \text{(A4)}$$

Equilibrium

$$\langle K \rangle = \frac{\langle k_a \rangle}{\langle k_d \rangle} = \frac{k_{a1}\psi_1 + k_{a2}\psi_2}{k_{d1}\phi_1 + k_{d2}\phi_2} \qquad \text{(A5)}$$

where ϕ_i represents are the mole fractions of the type-i radicals that can be calculated based on the long-chain assumption, such as $\phi_i = r_1 k_{p,2} f_1/(r_1 k_{p,2} f_1 + r_2 k_{p,1} f_2)$; ψ_i represents the mole fractions of the type-i dormant chains that can be calculated as the result of ATRP equilibrium, such as $\psi_1 = K_2\phi_1/(K_2\phi_1 + K_1\phi_2)$. When a uniform copolymer composition distribution along the polymer chain is targeted (that is, $F_1 =$ constant), all those rate coefficients remain unchanged during the copolymerization. Therefore, this kind of copolymerization kinetics is, in principle, similar to that of homopolymerization proposed by Fischer[38] and Goto and Fukuda.[3] However, we should also consider the volumetric variation caused by the monomer feeding in a semibatch operation.

At a certain total monomer conversion x, the distribution of comonomers between reactor and tank is illustrated in Table A1. N_{i0} is the initial mole of monomer i. The reaction volume $V = V_0(1 + \varepsilon x)$, where $V_0 = mw_1 N_{20} f_1/(\rho_{M1} f_2) + mw_2 N_{20}/\rho_{M2}$ is the reaction volume at $x = 0$. $V_f = N_0(mw_1 F_1 + mw_2 F2)/\rho_P$ is the final volume when all monomers are converted to polymer. $\varepsilon = (V_f - V_0)/V_f$ is the rate of volumetric variation.

The total moles of monomers in the semibatch system that includes reactor and feeding tank, N_M, decreases as

$$\frac{dN_M}{dt} = -\langle k_p \rangle [R](N_{1r} + N_{2r}) = -\langle k_p \rangle [R][N_{20}(1-x)/f_2]$$
$$= -(\langle k_p \rangle F_2/f_2)[R]N_0(1-x) = \langle k_p' \rangle [R]N_0(1-x) \qquad \text{(A6)}$$

or

$$\frac{dx}{dt} = \langle k_p' \rangle [R](1-x) \qquad \text{(A7)}$$

where $[R]$ is the total radical concentration ($[R_1] + [R_2]$) and $\langle k_p' \rangle = \langle k_p \rangle F_2/f_2$ is defined as the apparent propagation rate coefficient when a uniform copolymer composition is targeted. If the ATRP quasi-equilibrium is reached, and the cumulative concentration of dead chains is negligibly small compared to the concentration of living chains, we obtain

$$[R] = \frac{N_R}{V} \cong \frac{\langle K \rangle N_Q N_C}{N_Y V} \cong \frac{\langle K \rangle N_{I0} N_{C0}}{N_Y V} \qquad \text{(A8)}$$

Table A1. Distribution of Comonomer at Conversion x

Reactor		Tank	Total
Monomer 1 (mol^{-1})	$N_{20}\,(1-x)\,f_1/f_2$	$N_{10}\,(1-x)-N_{20}\,(1-x)\,f_1/f_2$	$N_{10}\,(1-x)$
Monomer 2 (mol^{-1})	$N_{20}\,(1-x)$	0	$N_{20}\,(1-x)$
Monomers converted into polymer (mol^{-1})	$N_0\,x$	0	$N_0\,x$

where the subscripts Q, C, and Y denote dormant chain, activator, and deactivator, respectively. N_{I0} and N_{C0} are the moles of initiator and activator at $t = 0$. The moles of deactivator, N_Y, are accumulated as the rate of

$$\frac{dN_Y}{dx} = \langle k_t\rangle[R]V/\langle k_p'\rangle(1-x) = \langle k_1\rangle\langle K\rangle N_{I0}N_{C0}/\langle k_p'\rangle N_Y(1-x) \tag{A9}$$

Integration of Eq. A9 yields

$$N_Y = \left[-2\langle k_t\rangle\langle K\rangle N_{I0}N_{C0}\ln(1-x)/\langle k_p'\rangle\right]^{1/2} \tag{A10}$$

Then, the molar fraction of dead chains is

$$N_{dead} = N_Y/N_{I0} = \left[-2\langle k_t\rangle\langle K\rangle N_{C0}\ln(1-x)/\langle k_p'\rangle N_{I0}\right]^{1/2} \tag{A11}$$

By inserting Eqs. A8 and A10 into Eq. A7, the following implicit form of polymerization rate can be obtained after integration:

$$t = \left[2\langle k_t\rangle V_0^2/\left(\langle k_p'\rangle^3\langle K\rangle N_{I0}N_{C0}\right)\right]^{1/2} \times \left[2(1+\varepsilon)z^3/\,3 + \varepsilon z\exp(-z^2) - \varepsilon\sqrt{\pi}\,\mathrm{erf}(z)/2\right] \tag{A12}$$

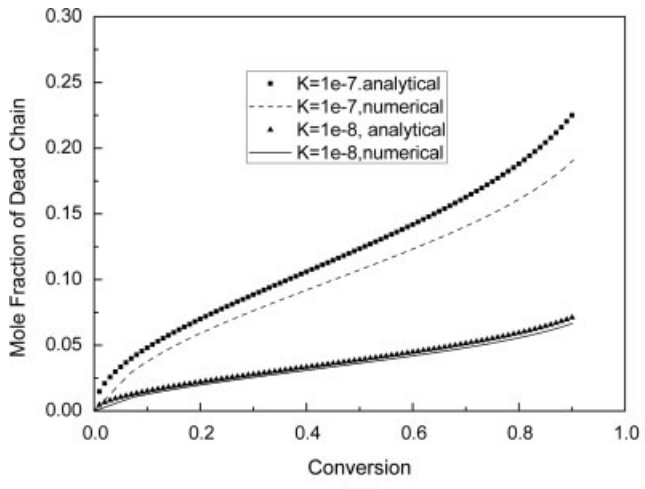

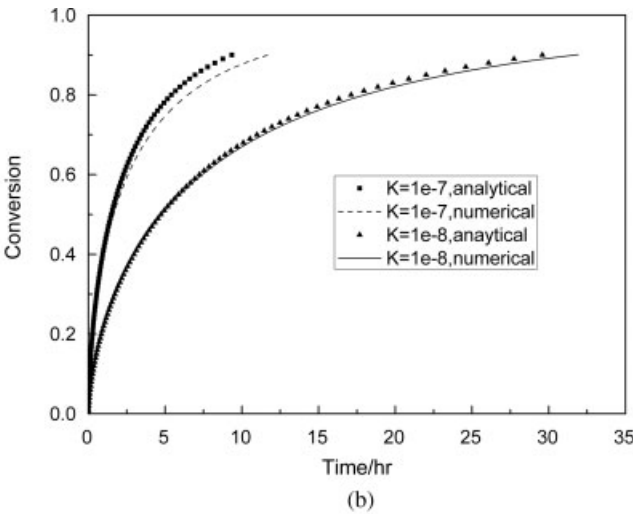

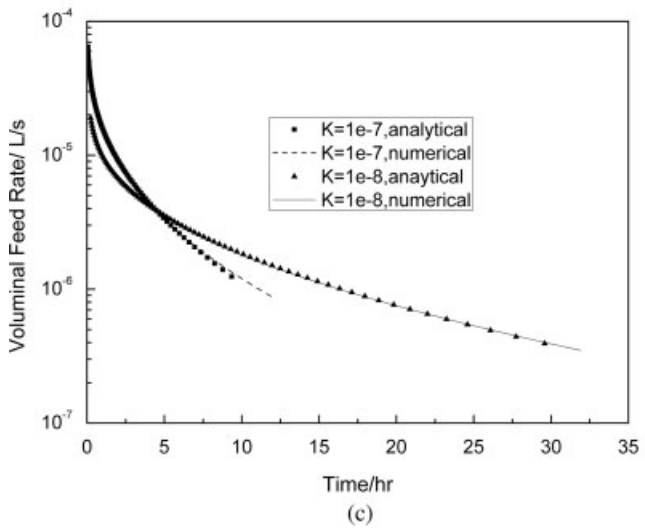

Figure A1. Comparison between the analytical and numerical solutions for System 2 at two ATRP equilibrium constants (10^{-7} and 10^{-8}).

(a) Molar fraction of dead chains vs. total monomer conversion, (b) total monomer conversion vs. reaction time, and (c) variation of volumetric feeding rate with time.

where $z = [-\ln(1 - x)]^{1/2}$. We can further solve the monomer feeding rate by combining Eqs. 2 and A7:

$$v_f = \left[\frac{\langle k_p' \rangle^3 \langle K \rangle N_{I0} N_{C0}}{2\langle k_t \rangle V_0^2}\right]^{1/2} \left[V_0 \varepsilon - N_0 \sum_i F_i M_{Wi} \left(\frac{1}{\rho_p} - \frac{1}{\rho_i}\right)\right] \times \left[\frac{1 - x}{(-\ln(1 - x))^{1/2}(1 + \varepsilon x)}\right] \quad \text{(A13)}$$

There are three assumptions involved in this derivation: (1) the long-chain assumption, (2) the establishment of ATRP equilibrium at an early stage, and (3) negligible fraction of dead chains.[38] The previous work demonstrated that the first two assumptions are valid in most ATRP systems, whereas the third assumption is questionable especially when $\langle K \rangle$ is large ($>10^{-7}$).[39] The analytical solutions are compared to numerical results as shown in Figures A1a, A1b, and A1c. Although the fraction of dead chains by the analytical estimation deviates from the numerical value when a large $\langle K \rangle$ value (10^{-7}) is used, the agreement between the analytical and numerical solutions in the polymerization rate and monomer feed profile are satisfactory.

The kinetics of semibatch copolymerization differs from its batch counterpart by the apparent propagating rate coefficient $\langle k_p' \rangle$ instead of $\langle k_p \rangle$ as illustrated in Eq. A7. The factor F_2/f_2 in the expression of $\langle k_p' \rangle$ denotes for the fraction of monomer distributed in reactor. $\langle k_p' \rangle$ is always smaller than $\langle k_p \rangle$ as $F_2/f_2 < 1$. Thus, the polymerization rate in a semibatch reactor is slower than that of a batch reactor because of the smaller apparent propagating rate coefficient. As the difference of r_1 and r_2 becomes large, F_2/f_2 further decreases, and a significant retardation occurs in the semibatch reactor as the case of System 3.

Manuscript received Aug. 13, 2006, and revision received Oct. 4, 2006.